Born–Oppenheimer dynamics using density-functional theory: Equilibrium and fragmentation of small sodium clusters

R. N. Barnett, Uzi Landman, Abraham Nitzan,[a] and Gunaretnam Rajagopal
School of Physics, Georgia Institute of Technology, Atlanta, Georgia 30332

(Received 5 September 1990; accepted 27 September 1990)

The properties of small neutral and positively charged sodium clusters and the fragmentation dynamics of Na_4^{++} are investigated using a simulation technique which combines classical molecular dynamics on the electronic Born–Oppenheimer ground-state potential surface with electronic structure calculations via the local spin-density functional method. Results for the optimal energies and structures of Na_n and Na_n^+ ($n \leqslant 4$) are in quantitative agreement with previous studies and experimental data. Fission of Na_4^{++} on its ground state Born–Oppenheimer potential-energy surface, following sudden ionization of selected configurations of an Na_4^+ (or Na_4) cluster, whose vibrational energy content corresponds to 300 K, is found to occur on a picosecond time scale. The preferred fission channel is found to be $Na_3^+ + Na^+$, with an interfragment relative translational kinetic energy of ~ 2 eV, and a vibrationally excited Na_3^+. The dynamics of the fragmentation process is analyzed.

I. INTRODUCTION

The evolution of energetic, structural, dynamic, and thermodynamic properties of matter as a function of the degree of aggregation (i.e., size of the system, or number of particles composing it) is of fundamental interest in diverse fields and for systems of widely varying length scales. The study of finite clusters of atomic and molecular constituents, in the size range bridging the molecular and condensed matter regimes, is an area of growing activity due to the development and proliferation of experimental techniques for the generation and probing of well-characterized size-selected clusters,[1] and the formulation and implementation of theoretical and computational methods which allow accurate predictions and elucidation of clusters' properties and phenomena.[2]

In addition to the inherent interest in the unique physical and chemical properties of atomic and molecular clusters, studies of the energetics, stability, and fragmentation of metal clusters (especially of free-electron metals) point to a close analogy between many properties of these clusters and those of atomic nuclei, despite the gross difference in the nature of binding in these systems. For example, the electronic shell structure and magic number stabilities,[3] quadrupolar surface deformations,[4,5] collective electronic excitations[3(a),6–13] (giant dipole, plasma resonances) and dissociation and fission (i.e., fragmentation of charged clusters, either spontaneously following ionization or by collisions with rare gas atoms) studied mostly in alkali-metal clusters[3(a),14–27] are properties whose nuclear analogs have long been studied.[28]

The energetics, stability, excitations, and optimal geometries of small alkali-metal clusters have been the subject of a large number of theoretical studies using high-level quantum-chemical computational techniques[13,29] and density functional (DF) methods[3(a),9,10,30–32] (within and beyond the spherical jellium approximation). In addition, jellium model calculations of the energetics of dissociation channels of neutral and charged sodium and potassium clusters have been made,[19–27] motivated by recent cluster photodissociation experiments.[14–16] The above studies were all for static ionic configuration (with the atomic geometry absent altogether in jellium calculations). Further insights into the properties of small alkali-metal clusters, in particular pertaining to the validity of the shell model predictions,have been recently obtained from classical dynamics simulations, on the ground state adiabatic electronic potential energy surface calculated via the local density functional method, in neutral sodium and mixed sodium–potassium clusters.[33]

The aims of our study are:

(i) Development of efficient methods for dynamical simulations of atomic and molecular clusters and other condensed matter systems, based on ionic dynamics on the ground state Born–Oppenheimer potential energy surface, determined via electronic structure calculations using the density functional theory.[34,35]

(ii) Application of the method to investigations of small neutral and charged metal clusters and of fragmentation dynamics.

Our simulation method is described in Sec. II. Energetic and structural results for Na_n and Na_n^+ ($n \leqslant 4$) clusters are presented in Sec. III A, and compared to previous theoretical studies and experimental results. In Sec. III B we demonstrate application of the simulation method to studies of the fragmentation dynamics of Na_4^{++}. These simulations indicate that starting from a Na_4^+ (or Na_4) cluster whose vibrational energy content corresponds to 300 K, spontaneous fragmentation, following ionization into the ground state potential energy surface of Na_4^{++}, occurs on a picosecond time scale. Starting from several configurations, dynamically generated for the parent cluster, the preferred fragmenta-

[a] Permanent address: Department of Chemical Physics, Weizmann Institute of Science, Rehovot 76100, Israel, and School of Chemistry, Tel Aviv University, Tel Aviv 69978, Israel.

 0021-9606/91/010608-09$03.00

tion channel is $Na_3^+ + Na^+$, with an interfragment relative kinetic energy of ~ 2 eV. While this fragmentation channel is the one predicted by examining the energies of the initial and final products for all the possible dissociation channels, we show that by restricting the initial state of an Na_4^+ (or Na_4) cluster to the equilibrium rhombus (D_{2h} symmetry) configuration, fragmentation on an energetically less favorable channel ($Na_2 + 2Na^+$) occurs. These results illustrate the importance of dynamical considerations in investigations of reaction dynamics. We summarize our results in Sec. IV.

II. METHOD

In principle, complete descriptions of static, dynamic, and thermodynamic physical and chemical properties and processes of materials are contained in solutions to the Schrödinger equation. However, for all but the most idealized models, such solutions are not possible without resorting to approximate methods, motivated by physical and practical (computational) considerations.

One of the pillars of modern quantum-theoretical treatments of materials is the Born–Oppenheimer (BO) approximation,[36] based on the time-scale separation between nuclear and electronic motion. Even within the BO framework, calculations for multielectron and nuclei system require further approximations. While high-level quantum-chemical computational techniques provide valuable information for small clusters of atoms (for selected nuclear configurations), they are not suitable for investigations of extended systems and of time-dependent phenomena which require repeated evaluation of the electronic energy along the trajectories of the nuclei.

Density functional theory,[34,35] and in particular local spin-density[37] (LSD) and the local density (LD) approximations,[34] provide accurate (although approximate) and practical methods of solution for quantum many-body problems and have become over the past two decades cornerstones of electronic structure calculations in condensed matter physics. The long conceived goal of combining nuclear molecular dynamics (with the nuclei treated classically) with ground-state electronic structure calculations via the LD method has been implemented successfully by Car and Parrinello[33] (CP) and used to investigate several systems.[33,38,39]

The evolution of systems of coupled quantum and classical degrees of freedom has been the subject of intensive investigations leading to the development of the path-integral[2(b)–2(d)] (PI) and time-dependent self-consistent field[2(a),2(c)] (TDSCF) methods. Adiabatic evolution on a single electronic potential energy surface (usually the ground state) using the TDSCF method is obtained by restricting the electron(s) to remain in a specified state along the dynamically evolving nuclear trajectories.[2(a),2(c),40–42] While most studies using this method were concerned with a single electron interacting with the media via pseudopotentials, an extension to a multielectron system (2–6 electrons), within the LSD scheme, has been made.[43]

The method which we have developed and used in our investigations of small sodium clusters and of the fragmentation dynamics of charged clusters, combines classical nuclear molecular dynamics with LSD electronic structure calculations, within the framework of the BO approximation. The approach is similar in spirit to other adiabatic simulations (e.g., those described in Ref. 43), though different in implementation. As such, this study is part of continued efforts aimed at the development of effective methods for adiabatic simulations of the dynamics of systems of coupled nuclear and electronic degrees of freedom.

In the LSD theory[37] the total electron density $\rho[\mathbf{r};\{\mathbf{R}(t)\}]$, for an N electron system, for a given nuclear configuration $\{\mathbf{R}(t)\}$, is given by

$$\rho[\vec{r};\{\vec{\mathbf{R}}(t)\}] = \sum_{j,\sigma} f_{j\sigma} |\psi_{j\sigma}[\vec{r};\{\vec{\mathbf{R}}(t)\}]|^2 \equiv \rho_\alpha(\vec{r}) + \rho_\beta(\vec{r}), \tag{1}$$

where $\sigma = \alpha$ or β ($\uparrow$ or $\downarrow$) is a spin label, and $0 \leqslant f_{j\sigma} \leqslant 1$ are the orbitals' occupation numbers. The orbitals $\psi_{j\sigma}$ are the single-particle self-consistent solutions (corresponding to eigenvalues $\epsilon_{j\sigma}$) of the Kohn–Sham (KS) LSD equations

$$H_\sigma^{\mathrm{KS}}[\vec{r},\rho(\vec{r}),\xi(\vec{r});\{\vec{\mathbf{R}}(t)\}]\psi_{j\sigma}[\vec{r};\{\vec{\mathbf{R}}(t)\}] = \epsilon_{j\sigma}\psi_{j\sigma}[\vec{r};\{\vec{\mathbf{R}}(t)\}], \tag{2a}$$

where

$$H_\sigma^{\mathrm{KS}}[\vec{r},\rho(\vec{r}),\xi(\vec{r});\{\vec{\mathbf{R}}(t)\}] = -\frac{\hbar^2}{2m}\nabla_{\vec{r}}^2 + V_{eI}[\vec{r},\{\vec{\mathbf{R}}(t)\}] + V_H[\rho(\vec{r}),\vec{r}] + V_{\mathrm{xc},\sigma}[\rho(\vec{r}),\xi(\vec{r})]. \tag{2b}$$

The first term in Eq. (2b) is the electron kinetic energy operator, V_{eI} is the electron–ion pseudopotential, and V_H and $V_{\mathrm{xc},\sigma}$ are the Hartree potential and local, spin-dependent, exchange-correlation potential $\{(\partial/\partial\rho_\sigma)E_{\mathrm{xc}}[\rho(\mathbf{r}),\xi(\mathbf{r})]\}$. The spin polarization function $\xi(\mathbf{r})$ is given by

$$\xi(\mathbf{r}) = [\rho_\alpha(\mathbf{r}) - \rho_\beta(\mathbf{r})]/\rho(\mathbf{r}). \tag{3}$$

In our calculations we have used the norm-conserving electron-sodium ion pseudopotential,[44] and for E_{xc} the interpolation formula of Vosko and Wilk.[45]

The solutions to the KS equations are obtained by us via the fast Fourier transform (FFT) technique, propagating in imaginary time with the split-operator method.[46,47] The manifold of KS orbitals is obtained by successive projections of lower (earlier determined) eigenstates $\psi_{j\sigma}$ ($j < m$), when determining $\psi_{m\sigma}$. The self-consistent solutions are achieved by iterating the process with the input electronic density for the $(i+1)$th iteration constructed from the densities of previous iterations (i.e., density mixing) according to Broyden's second method.[48] Convergence is tested by evaluating $I = \{\int d^3r[\rho^{(i)}(\vec{r}) - \rho^{(i+1)}(\vec{r})]^2\}^{1/2}$, where i is the iteration index, and is achieved when $I < 6\times10^{-8}$.

In the event of eigenvalue degeneracy, the above iterative scheme is unstable. To overcome this problem we use a Fermi-distribution function[49] for the occupation numbers $f_{j\sigma}$,

$$f_{j\sigma} = [\exp(\epsilon_{j\sigma} - \mu_\sigma)/k_B T_e + 1]^{-1}, \tag{4}$$

where the chemical potential μ_σ is obtained by solving the equation $N_\sigma = \Sigma_j f_{j\sigma}$ ($\Sigma_\sigma N_\sigma = N$). We found that choosing

$k_B T_e \approx 10^{-3}$ Hartree is adequate.

Our simulation procedure thus proceeds along the following steps:

(a) For a given ionic configuration, $\{\mathbf{R}(t)\}$, solve for the KS orbitals, as described above, and construct the electronic density $\rho[\mathbf{r},\{\mathbf{R}(t)\}]$.

(b) Propagate the positions and velocities of the ions $(I = 1,...,N_I)$ using the classical equations of motion

$$M\ddot{R}_I = -\nabla_{\mathbf{R}_I} V_{II}[\{\mathbf{R}(t)\}] - \int d\,\mathbf{r}\rho[\mathbf{r};\{\mathbf{R}(t)\}] \times \nabla_{\mathbf{R}_I} V_{eI}[\mathbf{r},\{\mathbf{R}(t)\}], \tag{5}$$

where V_{II} is the ion–ion Coulombic interaction and the second term on the right-hand side is the Hellmann–Feynman force of interaction between the ions and the electrons. The integration of the equations of motion, using the velocity Verlet algorithm,[50] yields a new ionic configuration $\{\mathbf{R}(t+\Delta t)\}$, where in our calculation $\Delta t = 0.025$–0.05 fs.

(c) Propagate the KS orbitals in real time, using FFT and the split operator technique, i.e.,

$$\psi_{j\sigma}[\mathbf{r};\{\mathbf{R}(t+\Delta t)\}] = \prod_{l=1}^{n_q} \exp\left(\frac{-iH_\sigma^{\mathrm{KS}}[\mathbf{r},\rho(\mathbf{r}),\xi(\mathbf{r});\{\mathbf{R}(t)\}]\delta t}{\hbar}\right) \times \psi_{j\sigma}[\mathbf{r};\{\mathbf{R}(t)\}]. \tag{6}$$

As evident from Eq. (6), due to the use of the split-operator technique, the real-time propagation, using a quantum time step $\delta t = \Delta t/n_q$, is repeated n_q times (typically $n_q = 10$) between classical steps. At the end of this process we have the (approximate) KS orbitals at time $t + \Delta t$.

(d) Using the KS orbitals at $t + \Delta t$, obtained in step (c), calculate $\rho[\mathbf{r};\{\mathbf{R}(t+\Delta t)\}]$ and the total energy $E(t+\Delta t)$.

(e) Check for energy conservation (this step is necessary because of the possibility of nonadiabatic transitions during the time evolution described above). If energy is conserved within a preset criterion (we use a deviation of $\pm 2.5\times 10^{-5}$ Hartree as a tolerance) we continue from step (b) above, using the updated electron density in Eqs. (5) and (6). Lack of energy conservation is evidence that the actual ground state can no longer be described by the (time evolved) original set of KS orbitals. In this case we continue from step (a), solving for a new set of self-consistent KS orbitals for the current ionic configuration. With the above choices of classical (Δt) and quantum (δt) time steps, instances of nonadiabaticity occur, for our system, on the average between (500–1000) Δt. In this context we note that the issue of nonadiabaticity depends on the nature of the electronic structure of the material (and the degree of aggregation). Thus, for semiconductors and insulators, the existence of gaps, much larger than the energy associated with thermal ionic motion, allows for substained adiabaticity for relatively long time periods. On the other hand, in metallic systems (as is our case) nonadiabaticity is ubiquitous.

The following two points should be noted:

(i) Since the KS Hamiltonian depends on the electronic density, which in turn is determined by the KS orbitals, events of degeneracy, or near-degeneracy, have to be considered. This can happen, for example, when the dynamical evolution of the ions results in configurations whose symmetries correspond to degenerate electronic states. These situations (which may also lead to crossing of energy levels) are dealt with effectively by including in the set of KS orbitals, which are self-consistently determined and propagated, a few orbitals above the initially highest occupied one, and using the Fermi-occupation function to determine the orbital's occupancies after each quantum propagation step.

(ii) Due to the unitarity of the quantum propagator [Eq. (6), and of the split-operator approximation to it] the orthogonality of the initial wave functions $\psi_{i\sigma}$ is maintained during the time evolution, thus avoiding time-consuming orthogonalization which enters other methods.[38]

III. ENERGETICS, STRUCTURES, AND FRAGMENTATION DYNAMICS OF SMALL SODIUM CLUSTERS

A. Energetics and structures

Using the simulation method described in the previous section, we have determined first the optimal structures and dissociation energies of Na_n and Na_n^+ ($n \leqslant 4$) clusters. All calculations were performed using a 32^3 FFT grid with a grid spacing of $0.75\,a_0$. The results of our calculations, along with those obtained by previous calculations[31] using the LSD method, and experimentally determined values[51–53] are given in Table I. The dissociation energy, D_e in Table I, for both the neutral and ionized clusters, is defined as the energy of the process $Na_n^{(+)} \rightarrow Na + Na_{n-1}^{(+)}$, and the energy E of a cluster is that corresponding to the optimal (minimum) energy geometry, with reference to the energy of the infinitely separated ions and valence ($3s$) electrons. Since the properties of sodium clusters are found to be rather insensitive to the nonlocal part of the ionic pseudopotential,[54] we restrict ourselves in these calculations to the $l = 0$ contribution, for which the ionization energy of a sodium atom is calculated to be 5.264 eV, compared to the experimental value[55] of 5.14 eV. To complete the description of our results we note that the optimal structure of Na_3 is an isosceles triangle C_{2v} symmetry) with an apex angle of 81.5°, which is a Jahn–Teller distortion of the equilateral triangle geometry. The latter geometry is found for the ionized Na_3^+ cluster. Both the Na_4 and Na_4^+ clusters possess a planar rhombic equilibrium geometry (D_{2h} symmetry), with the lengths of the long and short axes given in Table I.

The energies and structures obtained by us are in quantitative agreement with the results of previous calculations using the LSD method[31] (but with a different exchange-correlation potential) and with available experimental data.[51–53]

B. Fragmentation dynamics

Having discussed the equilibrium properties of small sodium clusters we turn to investigations of fragmentation dynamics following ionization. Recently, unimolecular dissociation channels of doubly charged $Na_n^{+\,+}$ clusters have been experimentally investigated,[16] near and above the critical size $n_c = 27$. In these studies it was found that on a time scale of 50 μs following photoionization of the neutrals by a

TABLE I. Calculated and experimental equilibrium configurations and energies of sodium clusters. Interionic distances (r_e), dissociation energies (D_e), total energies (E), and vibrational frequencies (ω_e). The lengths of the sides of the isosceles triangle equilibrium geometry of Na_3, and those of the long and short axes of the rhombus equilibrium geometry of Na_4 and Na_4^+, are given in parentheses.

	Na_2	Na_2^+	Na_3	Na_3^+	Na_4	Na_4^+
r_e (a_0)	5.546	6.546	(5.79,5.79,7.56)	6.26	(11.294,5.518)	(11.669,5.781)
	5.48[a]	6.42[a]	(5.7,5.7,7.1)[a]	6.0[a]	(11.114,5.5)[a]	(11.461,5.7)[a]
	5.818[b]	6.72[c]	...	...	...	...
D_e (eV)	0.8614	0.995	0.418	1.453	0.948	0.656
	0.91[a]	1.05[a]	0.40[a]	1.55[a]	0.63[a]	0.68[a]
	0.747[b]	0.991[d]	(0.378 – 0.527)[e]	1.30[d]	...	...
E (eV)	– 11.388	– 6.259	– 17.07	– 12.975	– 23.289	– 18.895
ω_e(cm^{-1})	148.9	119.9				
	173[a]	115[a]				
	159.1[b]	119[c]				

[a] Reference 31.
[b] Reference 51.
[c] Reference 52.
[d] Quoted in Ref. 31.
[e] Upper and lower bounds obtained from Ref. 53.

pulsed UV laser, doubly charged clusters of size $n \lesssim n_c$ fission asymmetrically (i.e., delayed fission into singly charged fragments). For larger clusters the main dissociation channel is the evaporation of a single neutral atom. In addition it was found that the charged fission products depart (recoil) with a kinetic energy of about 1 eV, and it was estimated that the Coulomb barrier for fission of $Na_{27}^{+\,+}$ is about 0.8 eV. These results emphasize the importance of dynamical considerations in studies of unimolecular decay of metastable charged clusters.

In our current studies we restricted ourselves to much smaller clusters than those investigated in the above mentioned experiments. Nevertheless these first simulations of the dynamics of a unimolecular dissociation process, evolving on a calculated adiabatic (BO) electronic potential energy surface, reveal the microscopic dynamics of a fission process occurring in $Na_4^{+\,+}$ on the picosecond time scale, as well as serve to illustrate the potential of the simulation method for further investigations of dynamical processes in clusters and other condensed matter systems.

In Tables II and III the energetics of dissociation channels of Na_4^+ and $Na_4^{+\,+}$ are shown. The values in the tables correspond to $\Delta = E_f - E_i$, where E_f is the equilibrium energy of the separated fragments and E_i is the equilibrium energy of the parent (initial) cluster (all energies calculated with reference to the infinitely separated ions and valence electrons). In the calculations of Δ in Table III, the rhombus configuration of minimum energy of $Na_4^{+\,+}$ was used.[56] In this structure the energy of $Na_4^{+\,+}$ is – 10.737 eV and the lengths of the long and short axes are 14.84 and 6.620 a_0, respectively. As seen from Table II all dissociation channels of Na_4^+ are endothermic. On the other hand, three of the dissociation channels of $Na_4^{+\,+}$ are exothermic (negative Δ values), with the asymmetric fission channel $Na_4^{+\,+} \rightarrow Na_3^+ + Na^+$ being the energetically favored one.

To simulate the fragmentation dynamics of $Na_4^{+\,+}$, we start from the optimal (zero temperature) geometry of Na_4^+ and assign to the sodium ions random velocities scaled such that the kinetic energy of each of the relevant six degrees of freedom (i.e., the cluster is prepared with zero angular and center of mass velocities) fluctuates about 300 K. The total potential energy $E_p = E_e + E_r$ (which includes the electronic energy E_e, and interionic repulsion energy E_r) and the kinetic energy of the Na_4^+ cluster, along a dynamically generated BO trajectory, are shown in Fig. 1(a), exhibiting variations due to the vibrational motion of the ions, as well as demonstrating conservation of energy (i.e., $E_p + E_k =$ constant). A decomposition of E_p, into the electronic (E_e) and interionic (E_r) contributions is shown in Fig. 1(b), and the time variation of the distance between the sodium ions

TABLE II. Dissociation channels of Na_4^+ and corresponding dissociation energies, Δ (in eV).

Dissociation channel	Δ (eV)
$Na_3^+ + Na$	0.66
$Na_2^+ + Na_2$	1.25
$Na_3 + Na^+$	1.825
$3Na + Na^{+\,+}$	3.1

TABLE III. Dissociation channels of $Na_4^{+\,+}$ and corresponding dissociation energies, Δ (in eV).

Dissociation channel	Δ (eV)
I. $Na_3^+ + Na^+$	– 2.24
II. $Na_2^+ + Na_2^+$	– 1.8
III. $Na_2 + 2Na^+$	– 0.65
IV. $2Na + 2Na^+$	0.21

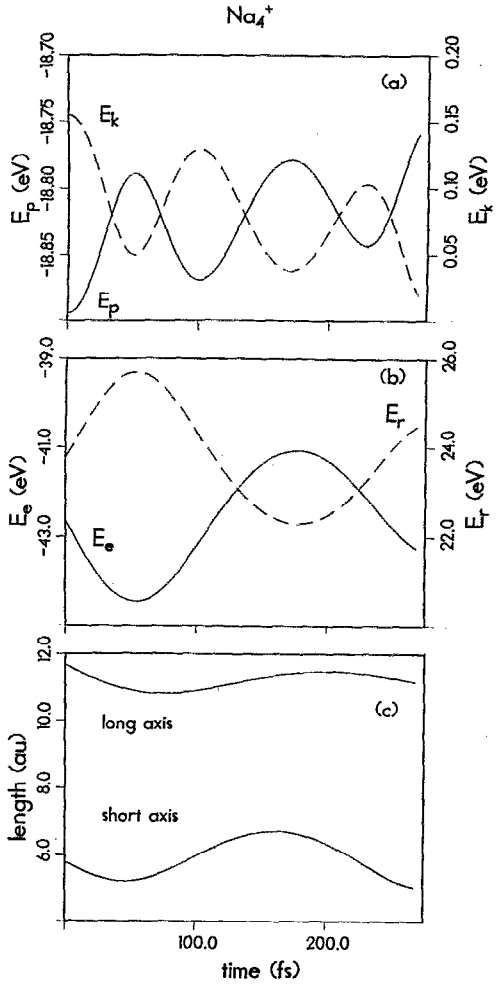

FIG. 1. Adiabatic (BO) simulation of a Na_4^+ cluster at 300 K. (a) Potential ($E_p = E_e + E_r$) and kinetic energies (E_k, dashed line) vs time (in fs); (b) electronic energy (E_e, solid line) and interionic repulsion (E_r, dashed line); (c) lengths of the long and short axes of the original rhombus configuration vs time.

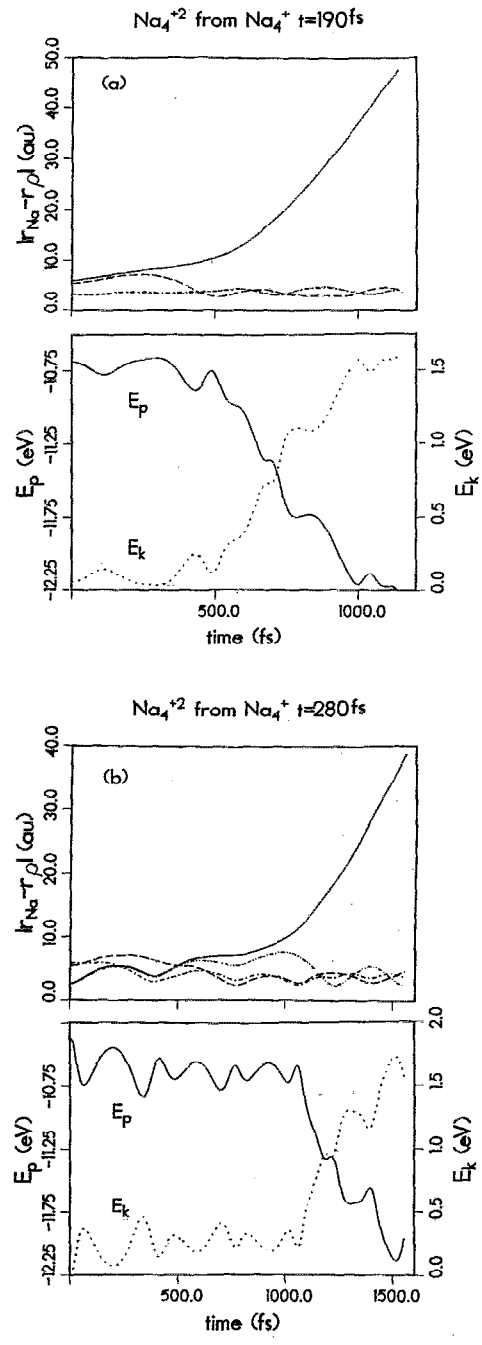

FIG. 2. Adiabatic simulations of the evolution of Na_4^{++} following ionization of Na_4^+ (see Fig. 1) at times $t_I = 190$ fs (in a) and $t_I = 280$ fs (in b). Shown, for each case, are the distances (in au) between each of the sodium ions and the center of the electron density ($|\mathbf{r}_{Na} - \mathbf{r}_\rho|$), and the potential ($E_p$, solid line) and kinetic (E_k, dashed line), vs time. Note that for $t_I = 190$ fs the Na^+ dissociates starts from the long axis of the original rhombus while for $t_I = 280$ fs the dissociating Na^+ starts from the original short axis.

located at the ends of the short and long axes of the initial rhombus configuration is shown in Fig. 1(c).

The initial states for simulations of the dynamics of Na_4^{++} were obtained by ionizing the Na_4^+ cluster (i.e., discarding the electron in the topmost occupied level) at several instances along the above trajectory. Following ionization the resulting Na_4^{++} cluster is allowed to evolve on its BO potential energy surface. We remark that in order to allow for all possible dissociation channels these calculations must be performed within the LSD scheme, since some of these channels involve products with unfilled electronic shells.

The temporal evolution of the system is shown in Fig. 2 for two trajectories of Na_4^{++}, following ionization of Na_4^+ at $t_I = 190$ and 280 fs (see Fig. 1). Shown in this figure are the time variations of the distances between each of the four sodium ions in the Na_4^{++} cluster from the center of the valence electron density ($|\mathbf{r}_{Na^+} - \mathbf{r}_\rho|$), and of the total potential and kinetic energies. As seen in both cases a fission of the cluster into Na_3^+ and Na^+ fragments occurs, where for the $t_I = 190$ fs event the Na^+ ion is initially one of the ions on the long axis of the cluster, while for the $t_I = 280$ fs event the product Na^+ is initially one of the short-axis ions. As seen, the onset of fission occurs ~0.6 and 1.2 ps, following ionization, in the two cases, respectively.

TABLE IV. Energetics of the fission reaction $Na_4^{++} \rightarrow Na_3^+ + Na^+$, ionizing a 300 K Na_4^+ cluster at different times, t_I (in fs), along its BO trajectory. The total energy of the Na_4^{++} produced from the parent Na_4^+ at time t_I, is given by $E_T(Na_4^{++})$. The internal potential and kinetic energies of the Na_3^+ fragment are denoted by $E_p^{(int)}(Na_3^+)$ and $E_k^{(int)}(Na_3^+)$, respectively, and their sum by $E_T(Na_3^+)$. The translational kinetic energies of the centers of mass of the fragments are given by $E_k^{(cm)}(Na_3^+)$ and $E_k(Na^+)$, and the residual, repulsive, interaction between the fragments at the end of the simulation is denoted by E_R. All energies are in eV.

t_I	$E_T(Na_4^{++})$	$E_T(Na_3^+)$	$E_p^{(int)}(Na_3^+)$	$E_k^{(int)}(Na_3^+)$	$E_k^{(cm)}(Na_3^+)$	$E_k(Na^+)$	E_R
78	− 10.238	− 12.228	− 12.699	0.471	0.317	0.952	0.721
190	− 10.653	− 12.723	− 12.825	0.102	0.376	1.128	0.566
280	− 10.403	− 12.371	− 12.641	0.270	0.321	0.962	0.685

Energetics of the fission processes for three ionization events (the two discussed above and an additional one initiated at an earlier t_I) are given in Table IV. We observe that at the end of the simulations the two fission products are separating with a kinetic energy $[E_k^{(cm)}(Na_3^+) + E_k(Na^+)]$ of ~ 1.3 eV. However, at the end of our simulations the two charged fission products are still interacting, predominantly via Coulomb repulsion. It is reasonable to expect that upon further separation this residual interaction energy (E_R in Table IV) will be converted mostly into kinetic recoil energy (from kinematical considerations E_R will be distributed in a ratio of 3:1 between the recoil kinetic energies of the Na_3^+ and Na^+ fragments, respectively.) Consequently, we estimate the total recoil energy of the fission process to be about 2.0 eV. In addition we note that the internal kinetic energy content of the Na_3^+ fragment corresponds to a vibrationally hot product. We remark, that the same fragmentation channel, with similar energetic characteristics, was obtained by us for other choices of initial configurations along the BO trajectory of the parent Na_4^+ cluster, as well as in simulations of the dynamics of dissociation of Na_4^{++} clusters which were obtained by doubly ionizing selected configurations from the BO trajectory of a neutral Na_4 parent cluster.

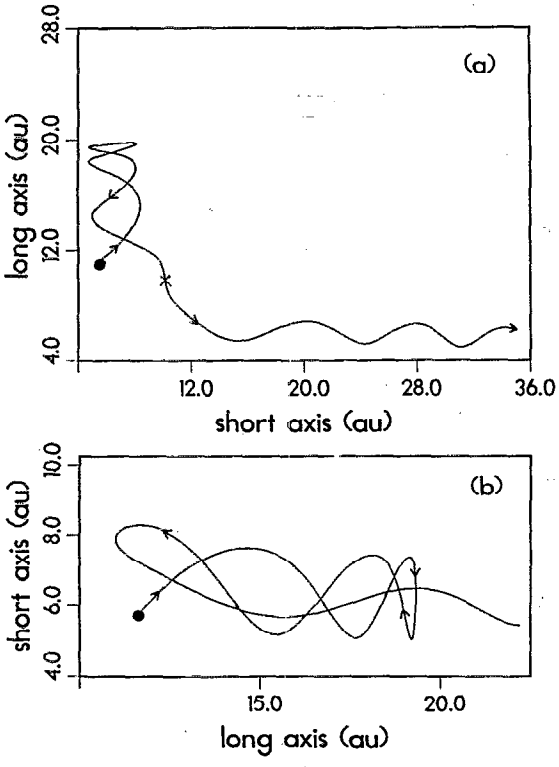

FIG. 3. Fission trajectories of a Na_4^{++} cluster obtained by double ionization of a Na_4 cluster from its equilibrium configuration (in a), and by single ionization of a Na_4^+ cluster from the equilibrium configuration (in b). Both fission processes yield $Na_2 + 2Na^+$. The starting rhombus configuration is marked by a dot, and the arrows guide the eye along the dissociation trajectory.

It is instructive at this stage to comment on other investigations, in which the initial parent (Na_4^+ or Na_4) clusters were chosen to be in their planar rhombus (D_{2h} symmetry) equilibrium (optimal) configurations. Ionization of the parent cluster, and dynamical evolution of the Na_4^{++} cluster on its BO surface, results in a fragmentation into a Na_2 molecule and two Na^+ ions (channel III in Table III). We note that this dissociation channel is not the energetically favored one, rather its occurrence is dictated by the symmetry of the initial state. From Table III we observe that the other exothermic (spontaneous) dissociation channels do not preserve the D_{2h} symmetry of the initial configuration.

The paths of the dissociation processes are illustrated in Fig. 3 [starting from Na_4 and Na_4^+, in Figs. 3(a) and 3(b), respectively]. We note that in the first stage, shown in both Figs. 3(a) and 3(b), the long axis of the rhombus elongates, and when becoming about 20 a_0, the ions at the end of this axis come to a turning point and then reverse the direction of their motion. In the first case [Fig. 3(a)] these two ions eventually recombine forming an Na_2 molecule, and the two ions which were originally at the ends of the short axis separate, moving in opposite directions, while in the second case [Fig. 3(b)] the two ions come back to a distance of $\sim 8\ a_0$ and then reverse the direction of their motion once again, resulting in dissociation.

These reaction paths are indicative of a barrier along the reaction coordinate, which in this case lies evidently along the long axis of the initial equilibrium rhombus structure. Indeed, the results shown in Fig. 4(a), where the total potential energy (electronic plus interionic repulsion) of the Na_4^{++} cluster is shown vs the length of the long axis, verify the existence of a barrier of ~ 0.14 eV along this reaction coordinate. [The results in Fig. 4 were obtained by calculating the energies of the equilibrium (optimal) structures of the Na_4^{++} cluster, while holding two sodium ions at fixed positions in opposite corners, thus forming an incrementally elongated rhombus.] The correlation between the lengths of

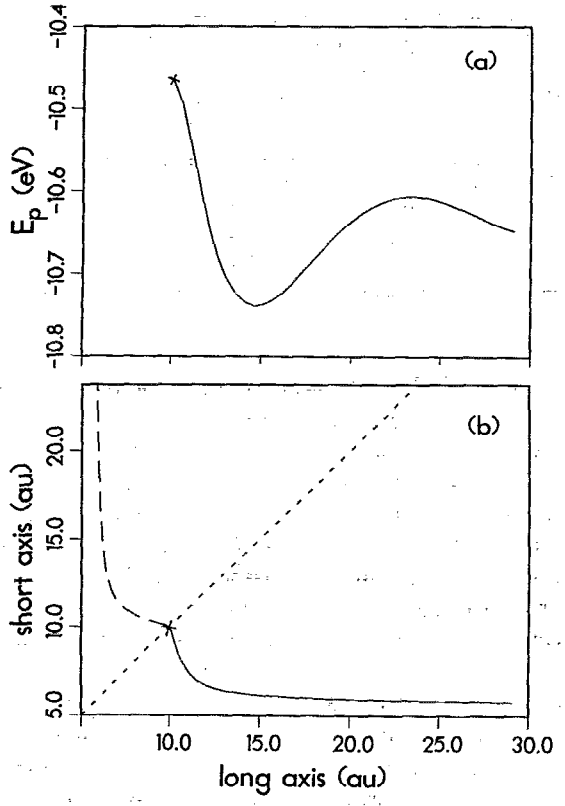

FIG. 4. (a) The potential energy (E_p) of Na_4^{++}, vs the length of the long axis of the rhombus, resulting from calculations in which the energy of the optimal configuration of the cluster is evaluated for an incrementally elongated rhombus (with the ions at the ends of the long axis held fixed at each distance and those on the short axis allowed to adjust such as to minimize the potential energy). A dissociation barrier of ~ 0.14 eV, along the long-axis reaction coordinate, is evident. (b) Variations of the short and long axes for the equilibrium rhombus configurations of Na_4^{++}. The square configuration of Na_4^{++} is marked by $\times$ in both (a) and (b). Energy in eV and lengths in au.

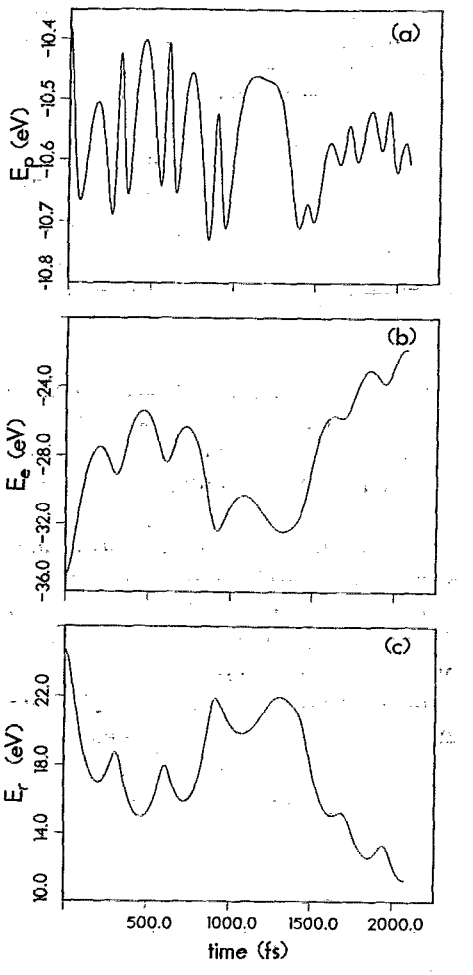

FIG. 5. Dissociation of Na_4^{++}, initiated by double ionization of the equilibrium Na_4 cluster. Shown vs time (in ps) are: (a) The potential energy ($E_e + E_r$); (b) the electronic energy (E_e); (c) the interionic Coulomb repulsion (E_r). Note the slowing down of the fluctuations in the total potential energy in (a), and occurrence of extrema in (b) and (c), at about 1.2 ps, corresponding to the reaction path passing through the unstable square configuration [see point marked $\times$ in Fig. 3(a)].

the short and long axes of the rhombus, corresponding to the equilibrium configurations of the cluster, is shown in Fig. 14(b).

Further information about the dissociation process of Na_4^{++}, obtained by ionizing the initial Na_4 cluster starting from its equilibrium configuration, is shown in Figs. 5 and 6. The total potential energy of the system vs time [shown in Fig. 5(a)] exhibits rapid fluctuations which slow significantly as the unstable square configuration is reached (at ~ 1.2 ps). This configuration is marked by an $\times$ in Figs. 3(a) and 4. We note that associated with this stage is a decrease in the electronic energy [Fig. 5(b)] and increase in the internuclear repulsion [Fig. 5(c)]. The energetics of this dissociation process may be summarized as follows: The total energy of the Na_4^{++} cluster, obtained by double ionization of the equilibrium (optimal) Na_4 cluster, is -10.389 eV. At the end of the simulation the Na_2 fragment is vibrationally cold (vibrational energy of 0.5×10^{-4} eV) and the total translational kinetic energy of the dissociating Na^+ ions is 0.968 eV (with the center of mass of the Na_2 fragment almost at rest).

Finally, contours (in the plane of the cluster) of the electronic charge density of Na_4^{++} at the initial state (just after ionization of the Na_4 cluster), at the point corresponding to the above square configuration (occurring ~ 1.2 ps after ionization), and at the end of the simulation, are shown in Fig. 6.

IV. SUMMARY

In this study we investigated the equilibrium properties of small neutral and charged sodium clusters (Na_n^+, $n \leqslant 4$), and the dissociation dynamics of Na_4^{++}, using simulations which combine local spin-density (LSD) calculations of the ground state electronic energy and density, with classical dynamics of the ions.

Our results (equilibrium energies and geometries) for small sodium clusters are in good agreement with previous LSD calculations and with experiments, when available.

Our calculations of the energetics of fragmentation of

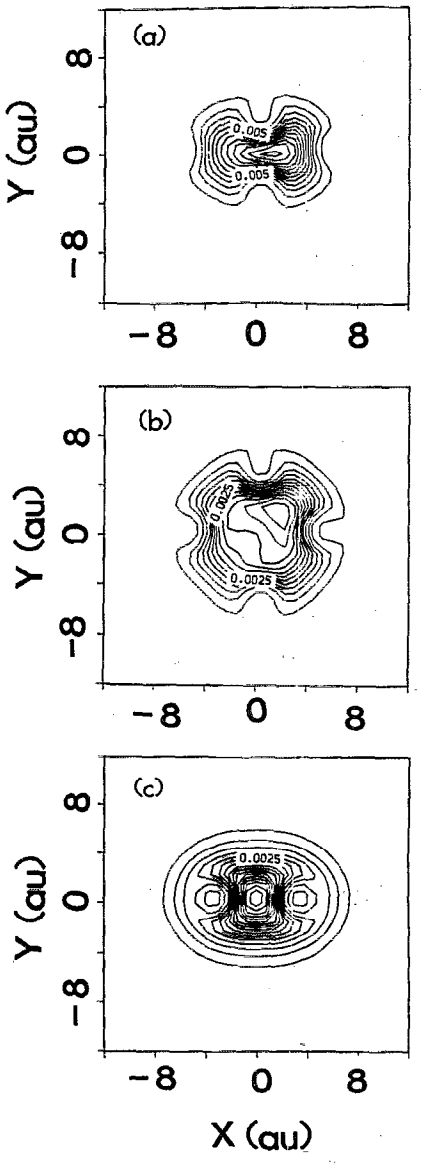

FIG. 6. Contours of the electron density of $Na_4^{+\,+}$ (in the plane of the planar cluster), obtained from the equilibrium Na_4 cluster, at different stages of dissociation. (a) Initial state of $Na_4^{+\,+}$ just following ionization; (b) at the square configuration [see point marked × in Fig. 3(a)]; (c) at the end of the simulation, where the contours are essentially those of the product Na_2 molecule, with the two dissociated Na^+ ions each at a distance of 17.5 a_0 from it.

Na_4^+ and $Na_4^{+\,+}$ show that while for Na_4^+ all dissociation channels are endothermic (see Table II), for $Na_4^{+\,+}$ three of the channels are exothermic (see Table IV), allowing for spontaneous fragmentation. Furthermore, starting from initial configurations, along the dynamically generated phase-space Born–Oppenheimer (BO) trajectory of Na_4^+ (or Na_4) at 300 K, our simulations show that upon sudden ionization, the resulting $Na_4^{+\,+}$ cluster fissions, on the picosecond time scale, on its ground-state potential-energy surface, yielding a vibrationally excited Na_3^+ fragment and an Na^+ ion, which recoil with a translational energy of ~ 2 eV. These results correlate with recent experimental studies of the asymmetric fission of larger doubly charged sodium clusters.

We also demonstrate that starting from the equilibrium (minimum energy, at 0 K) rhombus configuration of the parent cluster (Na_4 or Na_4^+), sudden (double or single) ionization, results in dissociation along an energetically less favorable channel, yielding $Na_2 + 2Na^+$, whose occurrence is dictated by the initial D_{2h} symmetry of the parent cluster. Moreover, we find that while the fission process, following sudden ionization from arbitrary chosen configurations (selected in our study from the BO phase-space trajectory of the parent cluster) is barrierless, dissociation of $Na_4^{+\,+}$, following ionization from the equilibrium geometries of Na_4 involves a barrier of ~ 0.14 eV along the reaction coordinate (elongation of one of the axes of the original rhombus). These results demonstrate the importance of dynamical considerations in investigations of reaction dynamics (unimolecular dissociation in particular) and caution against the exclusive selection of the equilibrium (minimum energy) configuration for the initial (parent) state.

In closing we remark that the simulation method which we described (see Sec. II) for investigation is of Born–Oppenheimer dynamics is an effective method for investigations of equilibrium and dynamical processes in multielectron and nuclei systems. Further applications of the method, to clusters and other condensed matter systems, are in progress.

ACKNOWLEDGMENTS

We thank Professors Robert L. Whetten and Mei-Yin Chou for stimulating discussions. This research is supported by the U.S. Department of Energy (DOE), Grant No. FG05-86ER-45234 (to U.L.) and by the US–Israel Binational Science Foundation and the Israel Academy of Science (to A.N.). Calculations were performed at the Florida State University Computing Center and at the National Energy Research Supercomputer Center, Livermore, California, through computer-time grants by DOE.

[1]See reviews in: (a) *Atomic and Molecular Clusters*, edited by E. R. Bernstein (Elsevier, Amsterdam, 1990); (b) *Elemental and Molecular Clusters*, edited by G. Benedek and M. Pacchioni (Springer, Berlin, 1988).

[2]See reviews by: (a) R. N. Barnett, U. Landman, G. Rajagopal, and A. Nitzan, Israel J. Chem. **30**, 85 (1990); (b) J. Jortner, D. Scharf, and U. Landman, in Ref. 1(b), p. 148; (c) U. Landman, in *Recent Developments in Computer Simulation Studies in Condensed Matter Physics*, edited by D. P. Landau, K. K. Mon, and H. B. Schuttler (Springer, Berlin, 1988), p. 144; (d) B. J. Berne and D. Thirumalai, Annu. Rev. Phys. Chem. **37**, 401 (1986); (e) R. Car, M. Parrinello, and W. Andreoni, in *Microclusters*, edited by S. Sugano, Y. Nishina, and S. Ohnishi (Springer, Berlin, 1987), p. 134.

[3](a) See review by W. A. de Heer, W. D. Knight, M. Y. Chou, and M. L. Cohen, Solid State Phys. **40**, 93 (1987); (b) For a recent investigation of the electronic shell structure in large metallic clusters and references to earlier studies see H. Gohlich, T. Lange, T.Bergmann, and T. P. Martin, Phys. Rev. Lett. **65**, 748 (1990); see also, J. L. Persson, R. L. Whetten, H.-P. Cheng, and R. S. Berry (preprint); (c) for recent work on cold sodium clusters and references to earlier studies, see E. C. Honea, M. L. Homer, J. L. Persson, and R. L. Whetten, Chem. Phys. Lett. **171**, 147 (1990).

[4]K. Clemenger, Phys. Rev. B **32**, 1359 (1985).

[5]W. Ekardt and Z. Penzar, Phys. Rev. B **38**, 4273 (1988).

[6]W. A. de Heer, K. Selby, V. Kressin, J. Masuri, M. Volhmer, A. Chatelain, and W. D. Knight, Phys. Rev. Lett. **59**, 1805 (1987).

[7]C. Brechignac, Ph. Cahuzac, F. Calier, and J. Leygnier, Chem. Phys. Lett. **164**, 433 (1989).

[8]C. R. C. Wang, S. Pollack, and M. M. Kappes, Chem. Phys. Lett. **166**, 26 (1990).
[9]M. J. Puska, R. M. Nieminen, and M. Manninen, Phys. Rev. B **31**, 3486 (1985).
[10]W. Ekardt, Phys. Rev. B **31**, 6360 (1985).
[11]D. E. Beck, Phys. Rev. B **35**, 7325 (1987).
[12]C. Yannouleas, R. A. Broglia, M. Brack, and P. F. Bortignon, Phys. Rev. Lett. **63**, 255 (1989); C. Yannouleas, J. M. Pacheco, and R. A. Broglia, Phys. Rev. B **41**, 6088 (1990).
[13]V. Bonacic-Koutecky, P. Fantucci, and J. Koutecky, Chem. Phys. Lett. **166**, 32 (1990); V. Bonacic-Koutecky, M. M. Kappes, P. Fantucci, and J. Koutecky, *ibid.* **170**, 26 (1990).
[14]See a review by O. Echt, in *Physics and Chemistry of Small Clusters*, edited by P. Jena, B. K. Rao, and S. N. Khanna (Plenum, New York, 1987), p. 623 and references therein.
[15]C. Brechignac, Ph. Cahuzac, F. Carlier, and J. Leyghier, Phys. Rev. Lett. **63**, 1368 (1989); C. Brechignac, Ph. Cahuzac, J. Leygnier, and J. Weiner, J. Chem. Phys. **90**, 1492 (1989).
[16]C. Brechignac, Ph. Cahuzac, F. Carlier, and M. de Frutos, Phys. Rev. Lett. **64**, 2893 (1990).
[17]For experimental studies of Pb_n^{+} $^{+}$ see: P. Pfau, K. Sattler, R. Pflaum, and E. Recknagel, Phys. Lett. A **104**, 262 (1984); W. Schulze, B. Winer, and I. Goldenfeld, Phys. Rev. B **38**, 12937 (1988).
[18]For experimental studies of fission of charged gold clusters see W. A. Saunders, Phys. Rev. Lett. **64**, 3046 (1990).
[19]B. K. Rao, P. Jena, M. Manninen, and R. M. Nieminen, Phys. Rev. Lett. **58**, 1188 (1987).
[20]C. Baladron, J. M. Lopez, M. P. Iniguez, and J.A. Alonzo, Z. Phys. D **11**, 323 (1989).
[21]G. Durand, J. P. Daudley, and J. P. Malrieu, J. Phys. (Paris) **47**, 1335 (1986).
[22]S. N. Khanna, F. Reuse, and J. Buttet, Phys. Rev. Lett. **61**, 535 (1988).
[23]S. Saito and M. L. Cohen, Phys. Rev. B **38**, 1123 (1988).
[24]M. P. Iniguez, J. A. Alonso, A. Rubio, M. J. Lopez, and L. C. Balbas, Phys. Rev. B **41** 5595 (1990).
[25]M. P. Iniguez, J. A. Alonso, M. A. Allen, and L. C. Balbas, Phys. Rev. B **34**, 2152 (1986).
[26]Y. Ishii, S. Ohnishi and S. Sugano, Phys. Rev. B **33**, 5271 (1986).
[27]S. Sugano, A. Tamura, and Y. Ishii, Z. Phys. D **12**, 213 (1989).
[28]A. Bohr and B. R. Mottelson, *Nuclear Structure* (Benjamin, London, 1975).
[29]For a review see: J. Koutecky and P. Fantucci, Z. Phys. D **3**, 147 (1986); Chem. Rev. **86**, 538 (1986); V. Bonacic-Koutecky, P. Fantucci, and J. Koutecky, Phys. Rev. B **37**, 4369 (1988); see also references in P. Fantucci, S. Polezzo, V. Bonacic-Koutecky, and J. Koutecky, J. Chem. Phys. **92**, 6645 (1990); I. Boustani, W. Pewestorf, P. Fantucci, V. Bonacic-Koutecky, and J. Koutecky, Phys. Rev. B **35**, 9437 (1987).
[30]J. L. Martins, J. Buttet, and R. Car, Phys. Rev. Lett. **53**, 655 (1984).
[31]J. L. Martins, J. Buttet, and R. Car, Phys. Rev. B **31**, 1804 (1985).
[32]F. Reuse, S. N. Khanna, V. de Coulson, and J. Buttet, Phys. Rev. B **41**, 11743 (1990).
[33]P. Ballone, W. Andreoni, R. Car, and M. Parrinello, Europhys. Lett. **8**, 73 (1989).
[34]See articles in *Theory of the Inhomogeneous Electron Gas*, edited by S. Lundqvist and N. M. March (Plenum, New York, 1983).
[35]W. Kohn and L. J. Sham, Phys. Rev. **140** A1133 (1965).
[36]M. Born and J. Oppenheimer, Ann. Phys. **84**, 457 (1927); M. Born and K. Huang, *Dynamical Theory of Crystal Lattices* (Oxford University, London, 1954).
[37]D. Gunnarson and B. I. Lundqvist, Phys. Rev. B **13**, 4274 (1976).
[38]R. Car and M. Parrinello, Phys. Rev. Lett. **55**, 2471 (1985); for details see R. Car and M. Parrinello, in *Proceedings of the NATO ARW*, NATO ASI Series (Plenum, New York, 1989).
[39]G. Gali, R. M. Martin, R. Car, and M. Parrinello, Phys. Rev. Lett. **62**, 555 (1989); R. Car and M. Parrinello, *ibid.* **60**, 204 (1988); see also Ref. 49(b), below.
[40]See review by P. J. Rossky and J. Schnitker, J. Phys. Chem. **92**, 4277 (1988).
[41]A. Selloni, P. Carenvali, R. Car, and M. Parrinello, Phys. Rev. Lett. **59**, 823 (1987).
[42]R. N. Barnett, U. Landman, and A. Nitzan, Phys. Rev. A **38**, 2178 (1988); J. Chem. Phys. **89**, 2242 (1988); **90**, 4413 (1989); **91**, 5567 (1989).
[43]E. S. Fois, A. Selloni, M. Parrinello, and R. Car, J. Phys. Chem. **92**, 3268 (1988); Phys. Scr. T **25**, 261 (1989).
[44]D. R. Hamann, M. Schluter, and C. Chiang, Phys. Rev. B **26**, 4199 (1982).
[45]S. H. Vosko and L. Wilk, J. Phys. C **15**, 2139 (1982); S. H. Vosko, L. Wilk, and M. Nusair, Can. J. Phys. **58**, 1200 (1980).
[46]M. D. Feit, J. A. Fleck, and A. Steiger, Comput. Phys. **47**, 412 (1982).
[47]See review by R. Kosloff, J. Phys. Chem. **92**, 2087 (1988).
[48]See discussion in D. Singh, H. Krakauer, and C. Wang, Phys. Rev. B **34**, 8391 (1986).
[49](a) See Ref. 23; (b) G. W. Fernando, G.-X. Qian, M. Weinert, and J. W. Davenport, Phys. Rev. B **40**, 7985 (1989).
[50]J. R. Fox and H. C. Anderson, J. Phys. Chem. **88**, 4019 (1984).
[51]K. K. Verma, J. T. Bahns, A. R. Rejei-Rizi, W. C. Stwalley, and W.T. Zemke, J. Chem. Phys. **78**, 3599 (1983).
[52]S. Leutwyler, T. Heinis, M. Jungen, H.-P. Harri, and E. Schumacher, J. Chem. Phys. **76**, 4290 (1982); S. Martin, J. Chevaleyre, S. Valignat, J. P. Perrot, M. Broyer, B. Chabaud, and A. Hoareau, Chem. Phys. Lett. **87**, 235 (1982).
[53]J. L. Gole, G. J. Green, S. A. Pace, and D. R. Presuss, J. Chem. Phys. **76**, 2247 (1982); J. S. Hayden, R. Woodward, and J. L. Gole, J. Phys. Chem. **90**, 1799 (1986).
[54]W. Andreoni (private communication); and tests on selected cases.
[55]*Molecular Spectra and Nuclear Structure*, edited by K. P. Huber and G. Herzberg (Van Nostrand/Reinhold, New York, 1979).
[56]We emphasize that this configuration was obtained by restricting the structure to be a rhombus, and minimizing with respect to the lengths of the short and long axes.